



## Note

# Equilibrium and kinetic analysis of methyl orange sorption on chitosan spheres

W. A. Morais, A. L. P. de Almeida, M. R. Pereira, J. L. C. Fonseca \*

Departamento de Química, Universidade Federal do Rio Grande do Norte, Campus Universitário, Lagoa Nova, Natal, RN 59078-970, Brazil

## ARTICLE INFO

## Article history:

Received 17 January 2008

Received in revised form 25 May 2008

Accepted 28 June 2008

Available online 5 July 2008

## Keywords:

Chitosan

Adsorption kinetics

Dyes

Adsorption isotherms

Pseudo-order kinetics

Hydrobeads

Effluent treatment

## ABSTRACT

Chitosan can be used as adsorbent in the treatment of effluents from the textile industry, especially for negatively charged dyes, due to its cationic polyelectrolyte nature. In this work, the sorption of a model dye, methyl orange, on chitosan hydrobeads is analyzed in terms of equilibrium and kinetic approaches. Equilibrium studies showed that dye adsorption had a mixed Freundlich–Langmuir behavior that had its Langmuir character increased as the pH was increased. In terms of adsorption kinetics, it was found to be of  $n$ th-pseudo-order, with fractional  $n$  increasing from  $\sim 2$  to  $\sim 2.5$  as pH and initial dye concentration in the continuous phase were increased. The increase in the apparent pseudo-order was related to changes in mathematical approximation for the solution of the sorption rate equation, which were the result of the decrease in the ratio (number of active sites for adsorption)/(number of adsorbate molecules).

© 2008 Elsevier Ltd. All rights reserved.

Adsorption-related phenomena are involved in a wide range of processes used in carbohydrate research, such as heterogeneous catalysis,<sup>1</sup> stabilization of colloidal dispersions,<sup>2</sup> biocompatibility,<sup>3</sup> and effluent treatment.<sup>4</sup> Adsorption in particulate systems has been used for heavy metal uptake,<sup>5</sup> as part of the treatment of pulp and paper mill wastewater,<sup>6</sup> and in the treatment of effluents from the textile industry.<sup>7</sup>

Chitosan (Fig. 1a) is a biomacromolecule obtained from the deacetylation of chitin, a mucopolysaccharide extracted from the shells of crustaceans.<sup>8</sup> It can be used as adsorbent for treatment of textile industry effluents<sup>9</sup> as well as for metal uptaking from water.<sup>10</sup> This natural linear copolymer consists of  $\beta$ -(1 $\rightarrow$ 4)-2-amino-2-deoxy-D-glucopyranose and  $\beta$ -(1 $\rightarrow$ 4)-2-acetamido-2-deoxy-D-glucopyranose units.<sup>11</sup> Apart from being biocompatible, it is a polyelectrolyte with polycationic character that, depending on pH, is able to interact with negatively charged molecules.<sup>12</sup>

Spectrophotometry has been employed to quantify chitosan, using the strong interactions that occur between dye molecules and this biopolymer.<sup>13</sup> A reasonable amount of work on the analysis of sorption of dyes on chitosan has been carried out, these works usually being divided into two approaches: one dedicated to the obtaining of adsorption isotherms and another one on the kinetic analysis of sorption.<sup>9,14,15</sup> Physically and chemically modified chitosan has also been used in some works: for example, Wang and Wang have employed chitosan/montmorillonite nanocomposite

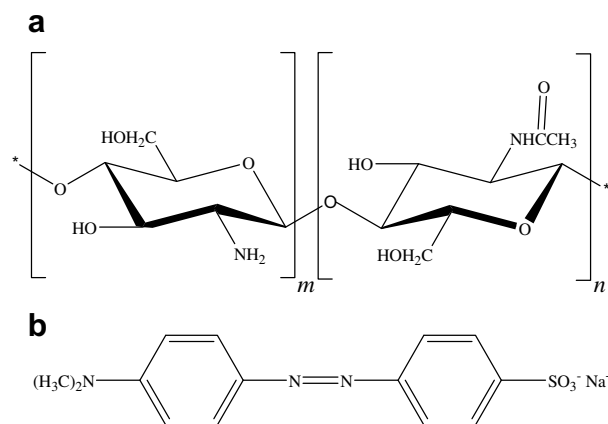


**Figure 1.** Chemical structures of (a) chitosan and (b) methyl orange. For the chitosan used in this work,  $m/(m+n) = 0.9$ .

particles in the sorption of Congo Red,<sup>16</sup> and Lima et al. have used chitosan chemically modified with succinic anhydride for methylene blue adsorption.<sup>17</sup>

Recently, some results on the sorption of methyl orange (Fig. 1b) as a model dye, on dry crosslinked chitosan particles have shown that the usual kinetics description as pseudo-second-order kinetics is not adequate to describe this particular sorption process.<sup>18</sup> It has also been found that diffusion-related phenomena govern the kinetics of sorption in these systems. The aim of the

\* Corresponding author. Tel.: +55 84 3215 3828x215; fax: +55 84 3211 9224.  
E-mail address: [jlcfonseca@uol.com.br](mailto:jlcfonseca@uol.com.br) (J. L. C. Fonseca).

present work is to perform experiments with crosslinked hydrobeads of chitosan and to compare the mechanism of sorption with the one observed with the dry crosslinked particles.

As the results of this note show, the produced chitosan spheres had average diameter around 2–3 mm, determined from digital camera pictures, using the UTHSCSA Image Tools for Windows, version 3.00. Figure 2 shows a set of particles used in this work.

Figure 3 displays data relating  $q_E$  (the mass of adsorbed dye per mass of chitosan) to  $C_E$  (the dye concentration in the continuous phase at equilibrium) at different values of pH. For pH 5, data were well adjusted to the Freundlich isotherm, expressed here as<sup>19</sup>

$$q_E = K_F C_E^{1/n_F}, \quad (1)$$

where  $n_F$  is the heterogeneity factor and  $K_F$  is a constant. Fitting of data related to pH 7 and pH 8 was better when using the Langmuir–Freundlich isotherm:<sup>20,21</sup>

$$q_E = \frac{q_{LF} a_{LF} C_E^{1/n_{LF}}}{1 + a_{LF} C_E^{1/n_{LF}}}, \quad (2)$$

where  $n_{LF}$  is the heterogeneity factor,  $q_{LF}$  is the saturation value of  $q_E$ , and  $a_{LF}$  is a constant, similar to the general constant  $a$  from Langmuir's isotherm.<sup>22</sup> In order to adequately describe the behavior of all the systems, it is interesting to define  $q_{max}$ , the limit mass of adsorbed dye per mass of chitosan, as continuous phase concentration tends to infinite, as

$$\frac{1}{q_{max}} = 0 \quad (3)$$

for Eq. 1, since in the Freundlich isotherm there is no formation of a limit adsorption layer, and

$$\frac{1}{q_{max}} = \frac{1}{q_{LF}} \quad (4)$$

for Eq. 2. Figure 4 shows how the values of  $a_{LF}$ ,  $n_{LF}$ , and  $1/q_{max}$  varied with pH. It is clear that, as pH was increased, sorption gained Langmuir character: the heterogeneity index,  $n_{LF}$ , tended to 1,  $1/q_{max}$  tending to a lower value, which must be related to the formation of a single dye monolayer; the increase in  $a_{LF}$ , by its turn, indicates

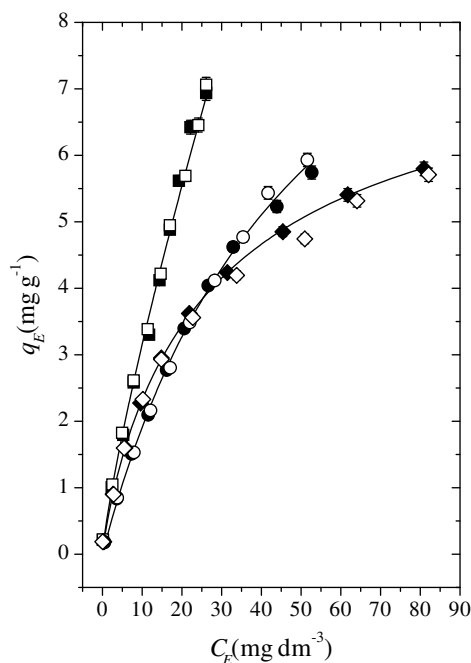


**Figure 3.** Mass of sorbed dye per gram of chitosan spheres,  $q_E$ , as a function of continuous phase concentration,  $C_E$ , for different values of pH. Squares: pH 5. Circles: pH 7. Diamonds: pH 8. The continuous lines represent Eq. 1 (Freundlich isotherm, pH 5), and Eq. 2 (Freundlich–Langmuir isotherm pH 7 and pH 8).

that chitosan tends to be saturated at lower values of  $C_E$ , as pH is increased (which is expected if the saturation tends to occur in the form of monolayer, as pH is increased).

These results are partially in agreement with the ones obtained with crosslinked chitosan in the form of dry powder.<sup>18</sup> The main difference is that data did not fit very well to the Freundlich isotherm at pH 5, which can be explained by the fact that the beads obtained in this work are highly hydrated, resulting in higher possibility of contacts between negatively charged dye molecules and

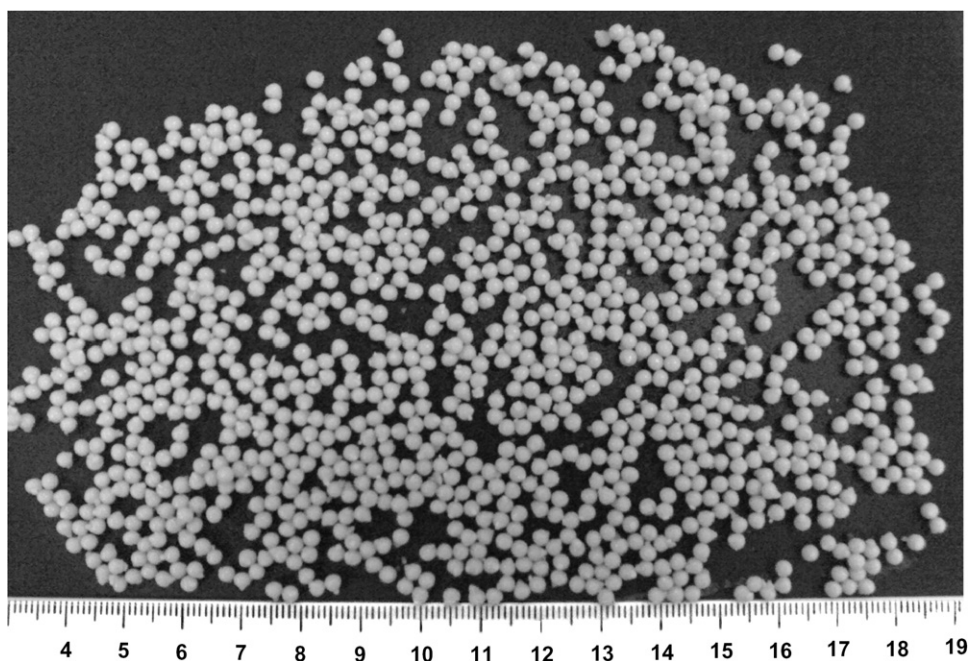


**Figure 2.** Crosslinked chitosan spheres obtained in this work. The rule in the picture has its scale in centimeters.

positively charged  $-\text{NH}_3^+$  sites from chitosan. At these conditions, the number of active sites must be so high that the tendency to saturation is minimal, resulting in a purely Freundlich character. As pH is increased, the number of these sites is reduced, resulting in an increase of Langmuir's character.

When mathematically describing sorption kinetics, dye concentration at the continuous phase,  $C$ , may be correlated to time,  $t$ , using the following models, as already described in a previous work:<sup>18</sup>

- Pseudo-first-order

$$C = C_0 + (C_0 - C_E)e^{-kt}, \quad (5)$$

where  $C_0$  is the dye concentration in the continuous phase prior to adsorption,  $C_E$  is the dye concentration at equilibrium, and  $k$  is the velocity constant. In terms of absorbance of the continuous phase,  $A$ , it follows that

$$A = A_0 + (A_0 - A_E)e^{-kt}, \quad (6)$$

where  $A_0$  is the absorbance of the continuous phase at  $t = 0$  (or the absorbance of the original solution), and  $A_E$  is the equilibrium absorbance of the continuous phase.

- Pseudo- $n$ th-order

$$C = C_E + \left[ \frac{1}{(C_0 - C_E)^{n-1}} + k(n-1) \left( \frac{V}{m_c} \right)^{n-1} t \right]^{1/(1-n)}, \quad (7)$$

where  $n > 1$  is the pseudo-order. In terms of continuous phase absorbance,  $A$ , it follows that

$$A = A_E + \left[ \frac{1}{(A_0 - A_E)^{n-1}} + k(n-1) \left( \frac{\alpha V}{m_c} \right)^{n-1} t \right]^{1/(1-n)}, \quad (8)$$

where  $\alpha$  is the constant slope of the calibration curve made with the dye solutions as described in Eq. 13.

Data from kinetic experiments were not well represented by Eq. 6 (pseudo-first-order) and data fitting to Eq. 8 yielded fractional pseudo-order values between 2 and 2.5, with correlation coefficients that were never lower than 0.99 (all data-fitting was carried out using nonlinear regression, as it was done with equilibrium data). Figure 5 shows a typical fit of  $A$  in relation to  $t$  for a particular value of pH and initial dye concentration,  $C_0$ .

Figure 6, which shows  $n$  as a function of pH and initial dye concentration,  $C_0$ , clearly indicates that  $n$  is bigger for higher values of pH and  $C_0$ . According to the interpretation given in terms of electrostatic interactions, as pH is increased, the number of active sites for adsorption is decreased. It could also be stated that the following ratio, named  $r_s$ , would decrease:

$$r_s = \frac{\text{number of active sites for adsorption at the surface of the adsorbent}}{\text{number of adsorbate molecules in the continuous phase}}. \quad (9)$$

Following this analysis, as  $C_0$  is increased (and pH is kept constant), the later ratio also decreases. In other words, according to Figure 6,  $n$  increases to values higher than 2 as  $r_s$  is decreased, despite the sorption kinetics in systems of this type has been described in the literature as pseudo-first-order<sup>23–26</sup> and pseudo-second-order.<sup>16,27,28</sup>

This deviation from observed pseudo-first and -second-order can be understood by analyzing the basic equation which relates the kinetics of  $n$ th-pseudo-order sorption:

$$\frac{dq}{dt} = k(q_E - q)^n = kq_E^n(1 - \theta)^n, \quad (10)$$

where  $q$  is the mass of sorbed dye per chitosan mass,  $q_E - q$  is proportional to the number of sites available to adsorption, and  $\theta = q/q_E$ . Since  $0 < \theta < 1$ , Eq. 10 can be expressed as a Taylor series around  $\theta = 0$  in the form of

$$\frac{dq}{dt} = kq_E^n \left[ 1 - n\theta + \frac{n(n-1)}{2}\theta^2 - \frac{n(n-1)(n-2)}{6}\theta^3 + \dots \right]. \quad (11)$$

If the number of sites is high enough so that its decay is very small (i.e.,  $\theta \ll 1$ ), only the first two terms of the sum might be used:

$$\frac{dq}{dt} \cong kq_E^n(1 - n\theta) \quad (12)$$

and the resultant behavior could be interpreted as pseudo-first-order kinetics (even for  $n > 2$ ). As the ratio active sites to adsorbate molecules,  $r_s$ , decreases, this equation ceases to work and higher terms of Eq. 11 are needed. The apparent pseudo-order of the kinetics increases, as observed in Figure 6.

The discussion above could also be used for a new insight on data previously obtained with dry crosslinked chitosan particles.<sup>18</sup> In that case, pseudo-order values were much higher than 2: a lower value of  $r_s$ , together with a more compacted polymer structure (which would make diffusion-related phenomena to rule sorption kinetics) would result in a higher deviation from the usual pseudo-second-order behavior.

Figure 7 shows data relating the velocity constant,  $k$ , to the pseudo-order of the kinetics,  $n$ . It can be seen that as  $n$  increases, there is an exponential increase in  $k$ . Since  $0 < (1 - \theta) < 1$ , an increase in  $n$  results in an exponential decrease in the term  $(1 - \theta)^n$ , so that  $k$  exponentially grows, in order that  $\frac{dq}{dt}$  has the same value in Eq. 10.

## 1. Experimental

Chitosan was purchased from Polymar Ltd (Brazil) and had a deacetylation degree of 90%. The polymer had viscosity-average molecular weight,  $\bar{M}_v \cong 2.3 \times 10^5 \text{ g mol}^{-1}$ , determined using the Mark-Houwink-Sakurada equation from viscometric data as described in the literature.<sup>29</sup> Methyl orange (PA, Vetec, Brazil), glutaraldehyde (25% aqueous solution, Vetec, Brazil), disodium phosphate,  $\text{Na}_2\text{HPO}_4$  (PA, Merck, Germany), monohydrated citric acid,  $\text{C}_3\text{H}_5\text{O}(\text{COOH})_3 \cdot \text{H}_2\text{O}$  (Vetec, Brazil), sodium hydroxide (PA, Labsynth, Brazil), and acetic acid (PA, Reagen Quimibrás Ltd, Brazil) were used as received.

### 1.1. Preparation of crosslinked beads

Chitosan was solubilized in a 4% (m/v) acetic acid solution, stirred for 24 h, filtered and pumped (Micronal peristaltic pump,

model B332 II, Brazil) through a supplied standard silicone tube with a nominal flow rate of  $1.92 \text{ mL min}^{-1}$ . A hypodermic needle ( $0.7 \times 25 \text{ mm}^2$ ) was plugged at the end of the tube so that regular formation of chitosan solution drops was possible. As the formed drops fell from the needle they were collected in a 10% (m/v) aqueous NaOH solution and chitosan spheres were promptly formed. The resultant beads were left resting for 24 h in the NaOH solution, washed several times with distilled water until water pH became neutral. Sphere crosslinking was carried out by using glutaraldehyde:<sup>30</sup> 50 g of chitosan spheres were added to 750 mL of a 2.5% (w/v) glutaraldehyde solution and the system was kept at room temperature for 24 h. The crosslinked spheres

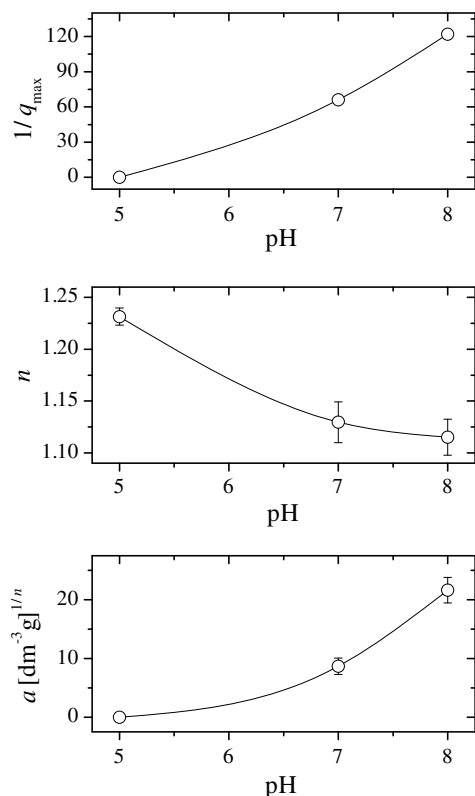


Figure 4. Parameters related to Eqs. 1–4 as a function of pH.

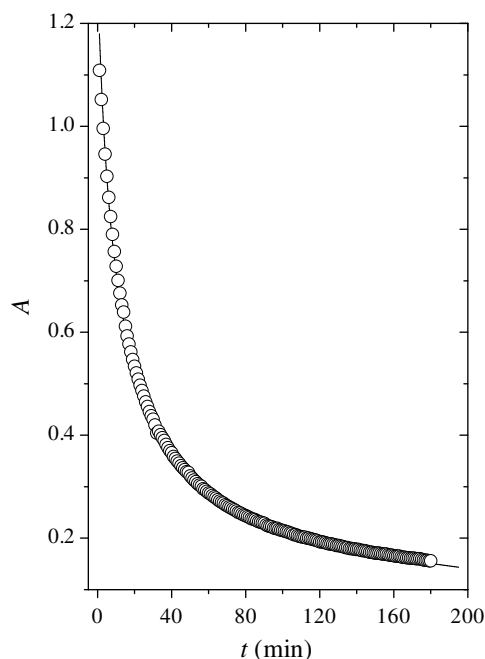


Figure 5. Continuous phase absorbance,  $A$ , as function of time,  $t$ , for dye sorption at pH = 8 and  $C_0 = 0.0155 \text{ g dm}^{-3}$ . At these conditions,  $r^2 = 0.99842$ ,  $n = 2.535 \pm 0.004$ , and  $k = (32 \pm 1) \times 10^3 \text{ min}^{-1}$ . The continuous line represents Eq. 8.

were continuously washed with distilled water, until a negative result for the Fehling test in water indicated the absence of glutaraldehyde.

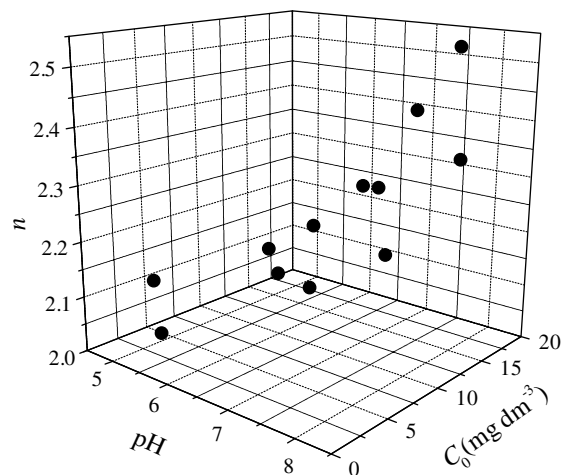


Figure 6. Pseudo-order  $n$  as a function of pH and initial dye concentration,  $C_0$ , obtained by fitting data to Eq. 8.

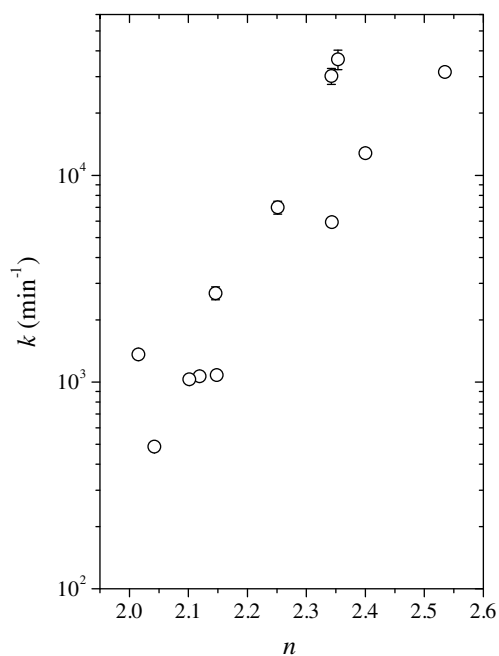


Figure 7. Velocity constant,  $k$ , as a function of  $n$  for data fitted to Eq. 8.

## 1.2. Equilibrium experiments

A mass  $m_c$  of ca. 2 g of chitosan spheres was weighted and added to a volume  $V = 20 \text{ mL}$  of a given dye solution and, after resting for 72 h at a temperature of  $(22 \pm 1)^\circ\text{C}$ , the continuous phase was separated from the spheres. The dye concentrations before and after sorption ( $C_0$  and  $C_E$ , respectively) were determined by UV-vis spectrophotometry (Thermoelectron Corporation, model Genesys 10uv), employing calibration curves previously built with the maximum absorption wavelength intensity for each value of pH, using

$$C = \alpha A, \quad (13)$$

where  $\alpha$  is a constant and the mass of sorbed dye per mass of chitosan at equilibrium conditions,  $q_E$ , was calculated:<sup>31</sup>

$$q_E = \frac{(C_0 - C_E)V}{m_c} \quad (14)$$

Sorption experiments were carried out with particles and solutions of methyl orange at different pH's, obtained using proper citric acid/disodium phosphate buffers, as described in a previous work.<sup>18</sup>

The resultant data were fitted to the following isotherms: Langmuir,<sup>22</sup> Freundlich,<sup>19</sup> Redlich–Peterson,<sup>32</sup> and Langmuir–Freundlich.<sup>20,21</sup> Kinniburgh has shown that direct nonlinear procedure is more adequate when fitting data from sorption experiments.<sup>33</sup> This procedure was applied to our data by the minimization of  $\chi^2$  function, via the Levenberg–Marquardt method, using the software Origin 7.5.<sup>34</sup>

### 1.3. Kinetic experiments

A mass  $m_c$  of 10 g of chitosan spheres was added to 100 mL of buffer solution and the system left to rest for 30 min. Afterwards, 70 mL of buffered dye solution was added to the system (so that the total volume of continuous phase was  $V = 170$  mL), which was placed in a shaker (Yellow Line OS 10 Basic, Ika, Germany) at 150 rpm. The dye concentration in the continuous phase was determined with intervals of 1 min by pumping it, using a peristaltic pump (Micronal, model B332 II, Brazil), to and from a quartz cell placed in a UV–vis spectrophotometer (Thermoelectron Corporation, model Genesys 10uv, USA), employing the same curves used for the equilibrium studies.

### Acknowledgments

The authors thank Brazil's Conselho Nacional de Desenvolvimento Científico e Tecnológico (CNPq), Ministério da Ciência e Tecnologia (MCT), Fundação Coordenação de Aperfeiçoamento de Pessoal de Nível Superior (CAPES), FINEP, CT-PETRO, and Pró-Reitoria de Pesquisa da Universidade Federal do Rio Grande do Norte (PROPESQ-UFRN) for financial support during the course of this work.

### References

- Asghari, F. S.; Yoshida, H. *Carbohydr. Res.* **2006**, *341*, 2379–2387.
- de Vasconcelos, C. L.; Pereira, M. R.; Fonseca, J. L. C. *J. Disper. Sci. Technol.* **2005**, *26*, 59–70.
- Roach, P.; Farrar, D.; Perry, C. C. *J. Am. Chem. Soc.* **2005**, *127*, 8168–8173.
- Westholm, L. J. *Water Res.* **2006**, *40*, 23–36.
- Babel, S.; Kurniawan, T. A. *J. Hazard. Mater.* **2003**, *97*, 219–243.
- Pokhrel, D.; Viraraghavan, T. *Sci. Total Environ.* **2004**, *333*, 37–58.
- Sanghi, R.; Bhattacharya, B. *Color Technol.* **2002**, *118*, 256–269.
- Neto, C. G. T.; Dantas, T. N. C.; Fonseca, J. L. C.; Pereira, M. R. *Carbohydr. Res.* **2005**, *340*, 2630–2636.
- Chatterjee, S.; Chatterjee, S.; Chatterjee, B. P.; Guha, A. K. *Colloids Surf., A* **2007**, *299*, 146–152.
- Webster, A.; Halling, M. D.; Grant, D. M. *Carbohydr. Res.* **2007**, *342*, 1189–1201.
- Beri, R. G.; Walker, J.; Reese, E. T.; Rollings, J. E. *Carbohydr. Res.* **1993**, *238*, 11–26.
- Saha, T. K.; Ichikawa, H.; Fukumori, Y. *Carbohydr. Res.* **2006**, *341*, 2835–2841.
- Wischke, C.; Borchert, H. H. *Carbohydr. Res.* **2006**, *341*, 2978–2979.
- Hu, Z. G.; Zhang, J.; Chan, W. L.; Szeto, Y. S. *Polymer* **2006**, *47*, 5838–5842.
- Kim, T. Y.; Cho, S. Y. *Korean J. Chem. Eng.* **2005**, *22*, 691–696.
- Wang, L.; Wang, A. Q. *J. Hazard. Mater.* **2007**, *147*, 979–985.
- Lima, I. S.; Ribeiro, E. S.; Airolidi, C. *Quim. Nova* **2006**, *29*, 501–506.
- Morais, W. A.; Fernandes, A. L. P.; Dantas, T. N. C.; Pereira, M. R.; Fonseca, J. L. C. *Colloids Surf., A* **2007**, *310*, 20–31.
- Freundlich, H. M. F. *Z. Phys. Chem.* **1906**, *57A*, 385–470.
- Sips, R. *J. Chem. Phys.* **1948**, *16*, 490–495.
- Sips, R. *J. Chem. Phys.* **1950**, *18*, 1024–1026.
- Langmuir, I. *J. Am. Chem. Soc.* **1918**, *40*, 1361–1403.
- Akkaya, G.; Uzun, I.; Guzel, F. *Dyes Pigments* **2007**, *73*, 168–177.
- Uzun, I. *Dyes Pigments* **2006**, *70*, 76–83.
- Yang, X. Y.; Al-Duri, B. J. *Colloid Interface Sci.* **2005**, *287*, 25–34.
- Wong, Y. C.; Szeto, Y. S.; Cheung, W. H.; McKay, G. *J. Appl. Polym. Sci.* **2004**, *92*, 1633–1645.
- Karadag, D.; Turan, M.; Akgul, E.; Tok, S.; Faki, A. *J. Chem. Eng. Data* **2007**, *52*, 1615–1620.
- Chiou, M. S.; Ho, P. Y.; Li, H. Y. *Dyes Pigments* **2004**, *60*, 69–84.
- Bezerril, L. M.; de Vasconcelos, C. L.; Dantas, T. N. C.; Pereira, M. R.; Fonseca, J. L. C. *Colloids Surf., A* **2006**, *287*, 24–28.
- Lin, Y. W.; Chen, Q.; Luo, H. B. *Carbohydr. Res.* **2007**, *342*, 87–95.
- de Vasconcelos, C. L.; Bezerril, L. M.; Dantas, T. N. C.; Pereira, M. R.; Fonseca, J. L. C. *Langmuir* **2007**, *23*, 1245–1252.
- Redlich, O.; Peterson, D. L. *J. Phys. Chem.* **1959**, *63*, 1024.
- Kinniburgh, D. G. *Environ. Sci. Technol.* **1986**, *20*, 895–904.
- Press, W. H.; Flannery, B. P.; Teukolsky, S. A.; Vetterling, W. T. *Numerical Recipes in Pascal: The Art of Scientific Computing*; Cambridge University Press: Cambridge, 1989.